Monte Carlo Calculations of Wall-to-Random-Bed View Factors: Impenetrable Spheres and Fibers

Josefina W. C. Tseng, Yong Xia, and William Strieder
Dept. of Chemical Engineering, University of Notre Dame, Notre Dame, IN 46556

Engineers often deal with random, hetergeneous void-solid systems, such as fluidized solid particles and various insulations and, in this context, the transport from a plane wall to a dispersed solid. For sufficiently large particles, view factors will describe the radiant heat transport (Siegel and Howell, 1981; Grace, 1982) between a gray diffuse wall and a finite size random gray bed, both of which have uniform temperature. Beyond radiation, Barron (1985) has pointed out that view factors can be used in low-pressure cryogenic insulation (Kaganer, 1969) for Knudsen void gas heat transfer. Wall-to-random-bed view factors will also predict mass-transfer penetration and deposition rates into thin fibrous or particulate supports for low-pressure sputtering processes (Wehner and Anderson, 1970).

In a previous article (Tseng and Strieder, 1990), plane-wall-to-adjacent-random-bed view factors were derived for several randomly dispersed solids: overlapping, equisized spheres and overlapping, identical, parallel long cylinders (parallel to the wall and to each other). Overlapping fiber models have been used to model various fiber beds for high-temperature chemical vapor deposition processes (Tomadakis and Sotirchos, 1991; Melkote and Jensen, 1989), and overlapping spheres have successfully described transport processes within silica gel (Van Eekelen, 1973). Impenetrable particles and fibers, however, are found more commonly in practice, and the corresponding view factors for nonoverlapping spheres and cylinders are also of interest. The straightforward statistics of the overlapping beds (Tseng and Strieder, 1990) yield analytical forms that need little or no numerical computation. In contrast, the nonoverlapping dispersions require an entirely different, computationally intensive approach. A realization of the random medium must be generated by direct Monte Carlo simulation. Subsequently, each realization is sampled for the desired quantity, and then an average is constructed over a number of realizations. The nonoverlapping simulation results are compared with the wall-to-random-bed view factors for the corresponding overlapping beds of spheres and fibers, and at lower solid fractions the curves coincide.

Correspondence concerning this work should be addressed to W. Strieder.
J. W. C. Tseng is presently with Rohm and Haas Co., Monomer Research, Spring House, PA 19477.

Wall-to-Sphere-Bed View Factors

Monte Carlo simulations were used to generate random nonoverlapping beds of spheres of radius a placed between two infinite parallel planes, Σ_0 and Σ_L, a distance L apart (Figure 1). N nonoverlapping spheres were initially placed in the positions (x_n, y_n, z_n) for $n = 1, \ldots, N$ within a simulation cell of dimensions $L \times W \times H$. For thicknesses L of $6a$, $10a$, $25a$ and $100a$, respectively, a maximum of 660, 2,066, 4,810 and 60,167 spheres were positioned into cells of volume $6a \times 32a \times 32a$, $10a \times 52a \times 52a$, $25a \times 52a \times 52a$ and $100a \times 200a \times 200a$. Since the view factors are asymptotically unity for smaller void fractions Φ:

$$\Phi = 1 - \frac{4\pi a^3}{3} \frac{N}{L \times W \times H}, \tag{1}$$

only sphere populations less than or equal to the maximum N needed to be considered. In those instances where the finite cell size could influence results, the cell size height and width were increased with a larger N, and the largest values are listed here. The cell was repeated in both the height and width directions to form an infinite slab of thickness L.

To randomize the array for larger void fractions, the spheres were placed directly into the cell in a random fashion, and those placements where spheres might overlap were rejected. This technique was effective only for void fractions from 0.93 to 1, where only a small fraction of the sphere placements were rejected. For the thickest case $L = 100a$, this covered the necessary void fraction range. For all other thicknesses and lower void fractions, that is, N from 1,292 to 4,810 for $L = 25a$, N from 516 to 2,066 for $L = 10a$, and N from 117 to 660 for $L = 6a$, the dispersion of spheres was randomized by the Metropolis Monte Carlo method (Hansen and McDonald, 1976). The N spheres were initially placed at the site locations (x_n, y_n, z_n) of a rectangular parallelopiped lattice. Each successive sphere $n = 1, \ldots, N$ was given a small random displacement to a new position, which was accepted or rejected according to whether the spheres overlap. If a sphere left the cell during a step of the simulation, another sphere entered the cell at the opposite side, thus preserving N. The test for sphere overlap included the sampling of the periodic images

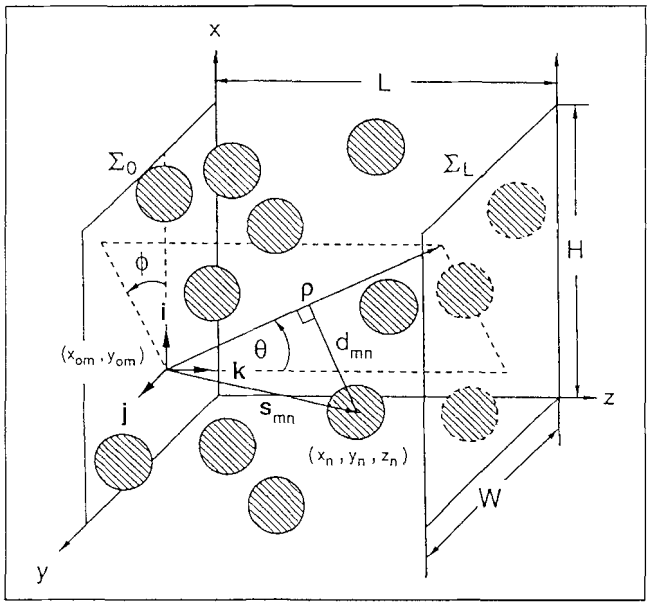

Figure 1. Variables in the Monte Carlo calculations of the directional free path probabilities and view factors for random, nonoverlapping sphere beds.

adjacent to the cell. If during a step, a sphere collided with one of the bounding walls Σ_0 or Σ_L, the sphere was elastically reflected back into the bed the distance it would have moved beyond the wall.

The W and H dimensions of the simulation cell are much larger than the range of sphere interaction $2a$; as a result, most of the spheres in the cell cannot overlap. The normal Monte Carlo procedure would waste much time during the displacement algorithm by needlessly testing for overlap that could not possibly occur. To avoid this, we divide up the cell into subcells of width $2a$, height $2a$ and length L. A subcell designation for each sphere is then created and updated as each sphere is moved. Then, to save computer time, the only spheres that must be checked for overlap with the sphere n are those in the subcell to which it belongs and the eight subcells encompassing the $2a \times 2a$ square.

The random displacement process was repeated over the N spheres numerous times. To ensure that the spheres were in equilibrium, 5×10^6 pre-equilibrium displacements were generated before the sampling of the realization began. A first sample was obtained at this point, and then at an interval of 0.5×10^6 displacements, successive samples were taken. The final results were over 200 realizations on average.

The systems considered in this work were hard-sphere fluids of different bulk densities located between semi-infinite parallel hard walls. The Metropolis Monte Carlo simulations were carried out for solid-sphere volume fractions from 0.08 up to 0.45. These values are sufficiently below the hard-sphere fluid-solid-phase transition at 0.495 to avoid any of the metastable behavior associated with this transition (Snook and Henderson, 1978; Hansen and McDonald, 1986). The view factors will be sensitive to the hard-sphere fluid structure near the edges of the suspension. To connect this simulation to previous studies and to test our techniques for generating an equilibrium sphere bed near a wall, we determined the sphere bed density profile $\rho(z)$ as a function of the coordinate z normal to the wall (Figure 1) for the largest plate separation $L = 25a$ of our Metropolis Monte Carlo simulations and the solid fraction 0.298. These results, given as the points in Figure 2, are compared with Monte Carlo values of $\rho(z)$ obtained by Snook and Henderson (1978) for the same solid fraction and essentially a semi-infinite slab. The results appear to be in good agreement.

The view factor F_{0L}, the fraction of radiation diffusely emitted from the plane Σ_0 that will travel an unobstructed straight line and arrive at Σ_L, is given by:

$$F_{0L} = \int d^2\rho \; P \; K \; (r, r') \tag{2}$$

where P is the probability that a vector ρ $[=(r'-r)]$ drawn from a randomly selected point r on Σ_0 to r' on Σ_L is unobstructed (Figure 1). The integration $d^2\rho$ is over the all plane wall surface elements on Σ_L. The differential view factor (Siegel and Howell, 1981):

$$K(r, r') = \begin{cases} -[\rho \cdot \eta(r)][\rho \cdot \eta(r')]/\pi\rho^4 & (r \text{ can see } r') \\ 0 & (\text{otherwise}) \end{cases} \tag{3}$$

is expressed in terms of ρ and $\eta(r)$, a unit normal located at r pointing away from the solid wall into the void volume of the bed. From its definition, the wall-to-bed view factor is:

$$F_{0b} = 1 - F_{0L} \tag{4}$$

For each of the Monte Carlo realizations, the free path probability P for nonoverlapping spheres must be computed numerically. For any direction θ, ϕ, origins $(x_{om}, y_{om}, 0)$ with $m = 1, \ldots, M$ were chosen at random for the vector ρ, the vector ρ was drawn across the slab (Figure 1), and P was the ratio of the number that reaches Σ_L without obstruction to the total number M. For any sphere n, we could determine the perpendicular distance d_{mn} from the line of action of ρ to the sphere center in terms of ρ and s_{mn}, the position vector of the

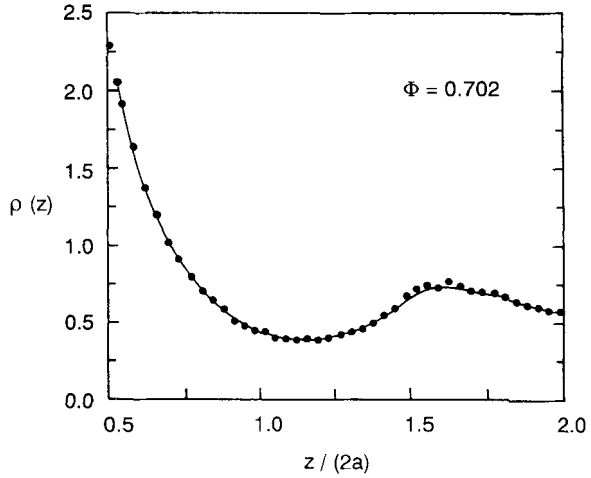

Figure 2. Density profiles for hard spheres near a hard wall.

Points give the Monte Carlo results from this work, and solid lines are based on simulations from Snook and Henderson (1978).

sphere center relative to the ρ origin (Figure 1). As long as d_{mn} was greater than the sphere radius:

$$d_{mn} = s_{mn}\,[1-(s_{mn}\cdot\rho)^2/(s_{mn}^2\rho^2)]^{1/2} > a \qquad (5)$$

blockage did not occur. The number M was adjusted experimentally by throwing vectors ρ and testing P at different intervals until it attained a constant value. For the bed geometries and bed sizes under consideration, 2,000 for M worked well.

Upon substitution of the differential view factor (Eq. 3) into the integral (Eq. 2), we found that K depended only on the colatitude angle θ, and integration over the azimuth ϕ gave:

$$F_{0L} = 2\int_0^{\pi/2} d\theta\; P(\theta)\;\sin\theta\;\cos\theta \qquad (6)$$

where $P(\theta)$ is the probability that any path from Σ_0 to Σ_L with colatitude angle θ is unblocked. For a bed of nonoverlapping spheres, $P(\theta)$ was computed at 17 colatitude angles between 0 and $\pi/2$, and the integral (Eq. 6) was evaluated by the three point Newton-Cotes composite method (Ralston and Rabinowitz, 1978).

Wall-to-bed view factors F_{0b} from Eq. 6 for F_{0L} and Eq. 4 are plotted as solid line curves in Figure 3 vs. the void fraction Φ for beds of nonoverlapping spheres of thickness $6a$, $10a$, $25a$, and $100a$. For comparison, the overlapping sphere bed view factors from Tseng and Strieder (1990) are also included as dashed curves. In all cases, the nonoverlapping curve lies above the overlapping case because the nonoverlapping model distributes the solid evenly and thus blocks more effectively. The greatest difference between the results of the two models are: 4.4% at $\Phi = 0.85$ for $L = 6a$; 3.7% at $\Phi = 0.88$ for $L = 10a$; and 1.9% at $\Phi = 0.94$ for $L = 25a$. For $L = 100a$, the curves are virtually coincident. At high void fractions above 0.92, overlap is no longer a factor and both models give the same results. For a given void fraction, the standard deviation of the Monte Carlo simulations, given as the bars on the solid curve in Figure 3, was at most 2.3% of the average value.

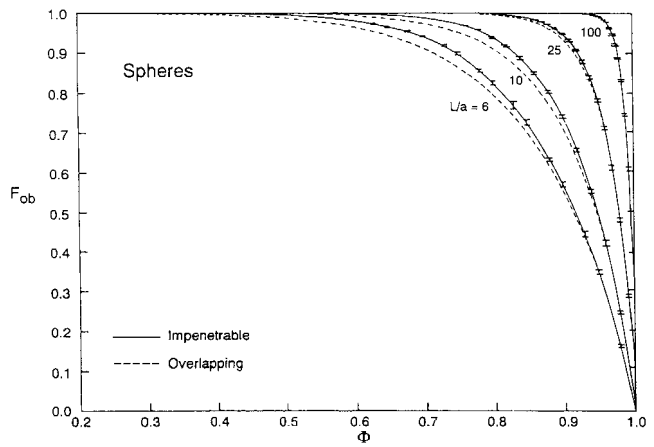

Figure 3. Wall-to-bed view factors F_{0b} for random, impenetrable sphere beds vs. bed void fraction Φ and thickness L/a, compared with view factors from overlapping sphere beds.

Bars indicate one standard deviation.

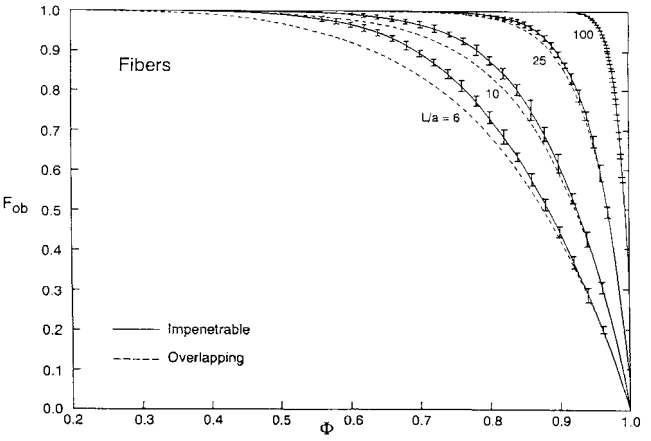

Figure 4. Wall-to-bed view factors F_{0b} for random, unidirectional, impenetrable fiber beds vs. bed void fraction Φ and thickness L/a, compared with view factors from overlapping fiber beds.

Bars indicate one standard deviation.

Furthermore, the greatest percent deviations occurred at high bed void fractions ($\Phi > 0.93$), where the average F_{0b} values already agreed with the exact overlapping sphere view factors from Tseng and Strieder (1990).

A fiber bed made of randomly placed, nonoverlapping identical cylinders aligned with central axes mutually parallel, and parallel to the bounding plane Σ_0 can be viewed from the side as a two-dimensional bed of circles or radius a. View factors from Monte Carlo simulations, very similar to those for the sphere beds (Xia, 1993), are plotted as solid curves in Figure 4. Standard deviations were 5.2% at maximum, and the largest deviations occurred for higher void fractions, where the correct results were already known from the convergence of solid and the dashed curve overlapping cylinder bed view factors.

Acknowledgment

Acknowledgment is made to the donors of the Petroleum Research Fund, administered by the American Chemical Society, for support of this research.

Notation

a = sphere or cylinder radius
d_{mn} = perpendicular distance from the line of action of ρ to the center of the nth sphere, Figure 1
F_{0L}, F_{0b} = wall Σ_0-to-wall Σ_L- and wall Σ_0-to-random-bed view factors
$K(r, r')$ = differential view factor, Eq. 2
$L \times W \times H$ = cell dimensions for the Monte Carlo simulation
M = number of random points selected on Σ_0
N = number of spheres within the cell
P = probability that ρ is unblocked
r = point on Σ_0 or Σ_L
s_{mn} = vector from the origin of ρ to the center of the nth sphere, Figure 1
x_{om}, y_{om} = randomly selected coordinates on Σ_0
x_n, y_n, z_n = Cartesian coordinates of nth sphere
$\eta(r)$ = normal vector at r
θ, ϕ = colatitude and azimuth angles
ρ = vector from a point r on Σ_0 to r' on Σ_L
Σ_0, Σ_L = planes $x=0$ and $x=L$
Φ = void fraction

Subscripts

m = index of a random point on Σ_0
n = sphere index

Literature Cited

Barron, R. F., *Cryogenic Systems*, Clarendon Press, Oxford, p. 388 (1985).

Grace, J. R., "Fluidized-Bed Heat Transfer," *Handbook of Multiphase Systems*, pp. 8-72, 8-52, and 8-53, G. Hestroni, ed., Hemisphere Publishing, New York (1982).

Hansen, J. P., and I. R. McDonald, *Theory of Simple Liquids*, Academic Press, New York (1976).

Kaganer, M. G., *Thermal Insulation in Cryogenic Engineering*, Israel Program for Scientific Translations, Jerusalem (1969).

Melkote, R. R., and K. F. Jensen, "Gas Diffusion in Random Fiber Substrates," *AIChE J.*, **35**, 1942 (1989).

Ralston, A., and P. Rabinowitz, *A First Course in Numerical Analysis*, McGraw-Hill, New York (1978).

Siegel, R., and J. R. Howell, *Thermal Radiation Heat Transfer*, p. 236, Hemisphere Publishing, New York (1981).

Snook, I. K., and D. Henderson, "Monte Carlo Study of a Hard-Sphere Fluid Near a Wall," *J. Chem. Phys.*, **68**, 2134 (1978).

Tomadakis, M. M., and S. V. Sotirchos, "Effective Knudsen Diffusivities in Structures of Randomly Overlapping Fibers," *AIChE J.*, **37**, 74 (1991).

Tseng, W. C., and W. Strieder, "View Factors for Wall to Random Dispersed Solid Bed Transport," *J. of Heat Transfer*, **112**, 816 (1990).

Van Eekelen, H. A. M., "The Random Spheres Model for Porous Materials," *J. Catal.*, **29**, 75 (1973).

Wehner, G. K., and G. S. Anderson, "The Nature of Physical Sputtering," *Handbook of Thin Film Technology*, pp. 3-25 and 3-26, L. I. Maissel and R. Glang, eds., McGraw-Hill (1970).

Xia, Y., "Wall to Random Bed Radiant Heat Transfer," PhD Thesis, Univ. of Notre Dame (1993).

Manuscript received July 8, 1991, and revision received Mar. 25, 1992.